Supporting Information for the article "Room-temperature negative differential resistance in single-atom devices"

Vladislav V. Shorokhov,[†,‡] Denis E. Presnov,[†,‡] Ilia D. Kopchinskii,[‡] Andrey A. Shemukhin,[‡,¶] Natalia S. Maslova,[‡] Vladimir N. Mantsevich,[†,‡] Artem S. Trifonov,[†,‡] Yuri A. Pashkin,[*,§] Oleg V. Snigirev,[†,‡] and Vladimir A. Krupenin[*,†,‡]

†*Quantum Technology Centre, Faculty of Physics, Lomonosov Moscow State University, Leninskie Gory, 1(2), Moscow, 119991, Russia.*

‡*Lomonosov Moscow State University, Faculty of Physics, Leninskie Gory, 1(2), Moscow, 119991, Russia.*

¶*D.V. Skobeltsyn Institute of Nuclear Physics, Lomonosov Moscow State University, Leninskie Gory, 1(2), Moscow, 119991, Russia.*

§*Department of Physics, Lancaster University, Lancaster LA1 4YB, UK*

E-mail: y.pashkin@lancaster.ac.uk; krupenin@physics.msu.ru

Phone: +7 495 9393014

Keywords

negative differential resistance, single-atom transistor, single-electron transistor, single dopant, nanobridge, silicon on insulator

Estimation of the characteristic energies of K dopants in Si

Potassium dopants are rarely used for implantation in silicon and silicon dioxide. A few implantation methods for K atoms were developed, for example, diffusive and ion accelerator implantation[1–4]. Potassium is an electrically active donor in silicon, however, the donor levels and their electrical properties are strongly dependent on the dopant location in the crystal lattice. The K dopant can be both interstitial and substitutional. It can form electrically inactive interstitial K-V complexes which are energetically more favourable due to the K neutral atom and K ion large atomic and ionic radius in comparison with silicon ($r_{K^0} = 1.93\,\text{Å}$, $r_{K^+} = 1.33\,\text{Å}$ and $r_{Si} = 1.17\,\text{Å}$) and hence high lattice stress. Potassium ions are most likely accommodated in the silicon lattice interstitially. The diffusion coefficient of potassium in silicon is $D_0 = 1.1 \times 10^{-8}\,\text{cm}^2/\text{s}$ and activation energy of diffusion is $E_{\text{diff}} = 0.8\,\text{eV}$[1,2]. The electrical conductivity of a potassium doped silicon surface decreases with annealing time[1–3], which is associated with the formation of electrically neutral K-V vacancy complexes in silicon.

It was shown earlier[1,2] that the potassium ionisation energy depends on the annealing temperature. For example, Hall measurements give the energy range $E_K = 0.04 - 0.115\,\text{eV}$ for annealing temperatures $620 - 720^\circ\text{C}$[1,2]. A different estimate of the two potassium energy levels is given by Sze[5]: $E_K = 0.26\,\text{eV}$ and $0.77\,\text{eV}$. This large variation in the energy values could be due to the different methods used for sample preparation and ion implantation.

Potassium dopant in silicon is a deep dopant. To estimate the effective potassium dopant Coulomb energy, effective electric capacitance and specific energy of inter-dopant electrostatic interaction, one can use the approach suggested by Glodeanu[6]. A more precise approach should use some *ab initio* calculations to determine these values. Following the Glodeanu approach one can fit the valence electron levels with using the effective core charge Z_{eff} and scaling parameter $\alpha \sim m^*/(m_e\varepsilon^2) \sim 0.01$, where m^* is the effective electron mass

in silicon and ε is the silicon permittivity. By using the variational model for single helium and lithium atoms[7], one can obtain expressions for their full energy

$$E_{\mathrm{He}} = -2(Z_{\mathrm{eff}} - 0.31)^2 \frac{\alpha e^2}{2a_0}, \qquad E_{\mathrm{Li}} = -\frac{9}{4}(Z_{\mathrm{eff}} - 0.46)^2 \frac{\alpha e^2}{2a_0} \tag{1}$$

We used a lithium variational model instead of potassium for estimation because of its simplicity and availability. Using (1), the energy of the first valence electron can be estimated as

$$E_1 = \left(\frac{1}{4} Z_{\mathrm{eff}}^2 - 0.84 Z_{\mathrm{eff}} + 0.29\right) \frac{\alpha e^2}{2a_0} \tag{2}$$

In equation (1) the specific electron-electron energy can be expressed as

$$u_{ee} = (0.7 Z_{\mathrm{eff}} - 0.16) \frac{\alpha e^2}{2a_0}. \tag{3}$$

From equation (2), for $E_{\mathrm{K}} = 0.26\,\mathrm{eV}$ one gets $Z_{\mathrm{eff}} \approx 5$, for $E_K = 0.11\,\mathrm{eV}$ the effective core charge value $Z_{\mathrm{eff}} \approx 4.1$. For a specific Coulomb energy for these values of $E_K = 0.26\,\mathrm{eV}$ one gets $u_{\mathrm{ee}} = 0.33\,\mathrm{eV}$ and $u_{ee} = 0.33\,\mathrm{eV}$ and $u_{\mathrm{ee}} = 0.27\,\mathrm{eV}$. This corresponds to the effective radii of the potassium dopant $r_{eff} = 2.2\,\mathrm{nm}$ and $r_{eff} = 2.7\,\mathrm{nm}$, respectively.

Using the expression for the electrostatic energy of two spheres of radius r that are separated by distance d[8]

$$W(q_1, q_2) = \frac{q_1 q_2}{\varepsilon} \left(\frac{1}{d} + \frac{2r^6}{d^7} + \frac{6r^8}{d^9} + \mathcal{O}\big(d^{-10}\big)\right), \tag{4}$$

one can estimate the inter-dopant specific interaction energy. For the implantation dose of $\sim 10^{13}\,\mathrm{cm}^{-2}$ and implantation depth of 20 nm, the average inter-dopant distance is estimated to be $d \sim 6\,\mathrm{nm}$. With these estimates, one obtains the electron-electron specific interaction energy for two dopants 0.02 eV and 0.021 eV, respectively.

Details of theoretical methods

This section provides a more detailed description of the theoretical model used to calculate the $I-V$ curves for dopant-based devices. Particular attention is paid to model parameterisation, which helps to improve fitting quality.

Theoretical model

To describe electron transport through localised states of dopant atoms, we employ a model of two two-level dopants connected in series. The second-quantised Hamiltonian of Anderson[9] type reads as follows

$$\begin{aligned}\hat{H} = &\sum_{\zeta\mathbf{k}\sigma} \varepsilon^{\zeta}_{\mathbf{k}}\, \hat{c}^{\zeta\dagger}_{\mathbf{k}\sigma}\hat{c}^{\zeta}_{\mathbf{k}\sigma} + \sum_{i=1}^{N}\sum_{\sigma=\uparrow,\downarrow} \varepsilon_{i\sigma}\, \hat{a}^{\dagger}_{i\sigma}\hat{a}_{i\sigma} + \sum_{i\zeta\mathbf{k}\sigma}\left(T^{\zeta}_{i\mathbf{k}\sigma}\hat{c}^{\zeta\dagger}_{\mathbf{k}\sigma}\hat{a}_{i\sigma} + T^{\zeta *}_{i\mathbf{k}\sigma}\hat{a}^{\dagger}_{i\sigma}\hat{c}^{\zeta}_{\mathbf{k}\sigma}\right) + \sum_{i\neq j}^{N} T_{ij\sigma}\, \hat{a}^{\dagger}_{i\sigma}\hat{a}_{j\sigma} \\ &+ \sum_{i} \tilde{U}_{ii}\big(\hat{n}_{i\uparrow} - \hat{1}n^{0}_{i\uparrow}\big)\big(\hat{n}_{i\downarrow} - \hat{1}n^{0}_{i\downarrow}\big) + \sum_{i<j}\tilde{U}_{ij}\big(\hat{n}_{i} - \hat{1}n^{0}_{i}\big)\big(\hat{n}_{j} - \hat{1}n^{0}_{j}\big), \end{aligned} \tag{5}$$

where fermionic operator $\hat{c}^{\zeta\dagger}_{\mathbf{k}\sigma}$ creates delocalised electron with quasi-wave vector $\mathbf{k}$, spin $\sigma \in \{\uparrow,\downarrow\}$ and energy $\varepsilon^{\zeta}_{\mathbf{k}} = \frac{\hbar^2\mathbf{k}^2}{2m} - \mu_\zeta - eV_\zeta$ in the conduction band of electrode $\zeta \in \{L,R\}$ (Fermi energy $\mu_\zeta \sim 5\,\mathrm{eV}$, effective mass $m \sim m_e$). Electrostatic potentials (such as eV_ζ) refer to the Fermi level of the grounded substrate, thus the actual Fermi levels of the source and drain electrodes are equal to $-eV_L$ and $-eV_R$, respectively. The fermionic operator $\hat{a}^{\dagger}_{i\sigma}$ creates an electron that occupies the i-th localisation site with spin σ and energy $\varepsilon_{i\sigma}$. Since the measured I-V curves exhibit two current peaks, we include two discrete energy levels in the spectrum of each dopant. Thus, the index i denotes $N=4$ levels with $i=1,2$ in the left dopant and $i=3,4$ in the right dopant. The spectra of both dopants can be shifted linearly with a common gate potential.

Elastic quantum-mechanical tunnelling events are introduced with the help of internal tunnel amplitudes $T_{ij\sigma}$ (processes $i\sigma \leftrightarrow j\sigma$) and external tunnel amplitudes $T^{\zeta}_{i\mathbf{k}\sigma}$ (processes $\zeta\mathbf{k}\sigma \leftrightarrow i\sigma$) which are derived from the geometric dimensions of the system as discussed

in subsection Tunnelling rates below. Inelastic tunnelling assisted by phonons or photons is neglected. Coulomb repulsion between localised electrons is represented by terms with Coulomb energies $\tilde{U}_{ij}$ and filling number operators $\hat{n}_{i\sigma} = \hat{a}^{\dagger}_{i\sigma}\hat{a}_{i\sigma}$ and $\hat{n}_i = \hat{n}_{i\uparrow} + \hat{n}_{i\downarrow}$. The Coulomb energies $\tilde{U}_{ij}$ are also derived from geometric dimensions in subsection Coulomb energies. The reference filling factors $n^0_{i\sigma}$ correspond to the electrically neutral electronic configuration of impurity atoms and significantly affect their discrete energy spectra $\varepsilon_{i\sigma}$ (see section Coulomb energies as well). Furthermore, discrete energy levels $\varepsilon_{i\sigma}$ are subject to classical fluctuations originating from background charge noise and the discarded electron-phonon interaction. We sample these fluctuations as discussed in subsection Effective local temperature and classical fluctuations.

The scalable `FORTRAN` implementation[10] of the non-equilibrium diagram technique equations is used to calculate the stationary electric current for the given bias and gate voltages. The general self-consistent calculation iteratively refines electronic filling factors until each of the stationary retarded and lesser Green's functions (their Fourier images) converges to its value, corresponding to the stable solution of self-consistent simultaneous Dyson and Keldysh equations:

$$G^R_{ij\sigma}(\omega) = \Big[\hat{G}^{0R}_{\cdot\cdot\sigma}(\omega)^{-1} - \hat{\Sigma}^{RT}_{\cdot\cdot\sigma}(\omega) - \hat{\Sigma}^{RC}_{\cdot\cdot\sigma}(\omega)\Big]^{-1}_{ij}, \quad G^<_{ij\sigma}(\omega) = \sum_{i'j'} G^R_{ii'\sigma}(\omega)\,\hat{\Sigma}^{<T}_{i'j'\sigma}(\omega)\,G^A_{j'j\sigma}(\omega), \tag{6}$$

where $G^{0R}_{ij\sigma}(\omega) = \delta_{ij}/(\hbar\omega - \varepsilon_{i\sigma} + i0)$, the stationary advanced Green's function $G^A_{ij\sigma}(\omega) = \big[G^R_{ji\sigma}(\omega)\big]^*$ and tunnel and Coulomb interactions reside in the self-energies $\Sigma^{RT}_{ij\sigma}(\omega), \Sigma^{<T}_{ij\sigma}(\omega)$ and $\Sigma^{RC}_{ij\sigma}(\omega)$, respectively (see[10] for details). Once equations (6) are solved numerically, one evaluates the expression for the electric current through the device,

$$I = \frac{e}{\hbar}\int \frac{\mathrm{d}(\hbar\omega)}{2\pi} \sum_{\sigma} 4\,\mathrm{Tr}\Big(\hat{G}^R_{\cdot\cdot,\sigma}(\omega)\,\hat{\Gamma}^L_{\cdot\cdot,\sigma}\,\hat{G}^A_{\cdot\cdot,\sigma}(\omega)\,\hat{\Gamma}^R_{\cdot\cdot,\sigma}\Big)\big[f^0_L(\hbar\omega) - f^0_R(\hbar\omega)\big], \tag{7}$$

which is obtained in the standard wideband approximation with the tunnelling rates $\Gamma^{\zeta}_{ij\sigma} \simeq$

$\pi\nu_\zeta^0(-eV_\zeta)\left|T^\zeta_{i|\mathbf{k}_F|\sigma}T^{\zeta*}_{j|\mathbf{k}_F|\sigma}\right|$, transversal density $\nu_\zeta^0(\hbar\omega)\,[1/\mathrm{eV}]$ of delocalised states and Fermi distribution functions $f_\zeta^0(\hbar\omega) = \left[1+\exp\left(\frac{\hbar\omega+eV_\zeta}{k_BT_\zeta}\right)\right]^{-1}$. The formalism of NDT allows for different temperatures k_BT_ζ of the electrodes. We set them equal $k_BT_L = k_BT_R = k_BT$, although the effective temperature k_BT is calculated self-consistently and accounts for self-heating of the structure due to the high density of the dissipated power. Subsection Effective local temperature and classical fluctuations defines the self-consistent equation for k_BT and clarifies the way it affects the averaging process of classical fluctuations for $\varepsilon_{i\sigma}$.

Model parameterisation

In this subsection, we briefly discuss the parameterisation of the tunnel amplitudes $T_{ij\sigma}$, $T^\zeta_{i\mathbf{k}\sigma}$ and Coulomb energies $\tilde{U}_{ij\sigma}$ via the geometric dimensions of the structure examined. Without this parameterisation, one would deal with a large number ($\sim N^2$) of the free energy parameters that inhibit predictive capability of the model. Therefore, we have reduced the number of free parameters to improve this capability and simplified the fitting process for I-V characteristics.

Tunnelling rates

We introduce a single free parameter for both the internal and external tunnel amplitudes: the common tunnel energy scale $B_0 = 2.5\,\mathrm{meV}$. The amplitude of any tunnelling process is expressed as B_0 multiplied by the quantum-mechanical transparency τ of the corresponding potential barrier. The barrier transparency is determined by its shape, which we approximate using piecewise linear one-dimensional functions (*e.g.*, energy diagram in Figure 4, the main text).

The linearity of the barrier shape (as in Figure 1) allows for the analytical calculation of its transparency using the Airy special functions,

$$\tau_\rightarrow(\varepsilon_i) = \frac{4|k_{iA}k_{iB}|/(\pi J)^2}{\left|\mathsf{W}[\mathrm{Ai},\phi^-_{iA}](x_A)\,\mathsf{W}[\phi^+_{iB},\mathrm{Bi}](x_B) \;+\; \mathsf{W}[\mathrm{Bi},\phi^-_{iA}](x_A)\,\mathsf{W}[\mathrm{Ai},\phi^+_{iB}](x_B)\right|^2}, \qquad (8)$$

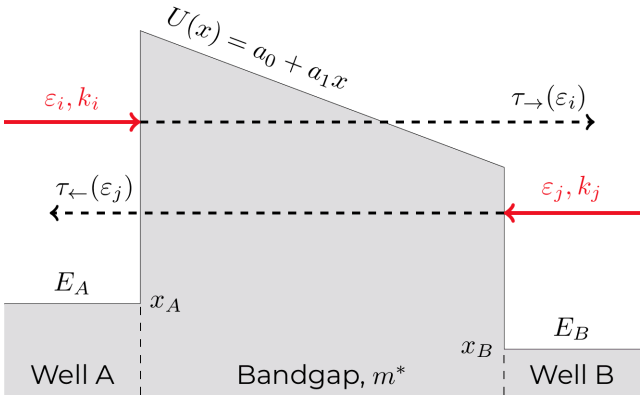

Figure 1: Transparencies of a linear potential barrier

where the electron wave vectors are $k_{iA} = \sqrt{2m(\varepsilon_i - E_A)}/\hbar$, $k_{iB} = \sqrt{2m(\varepsilon_i - E_B)}/\hbar$. One of the wells in Figure 1 may represent the conduction band of an electrode. The factor $J = \left(2a_1 m^*/\hbar^2\right)^{\frac{1}{3}}$ appears due to the change in variable $\xi(x)$ when solving the Schrödinger equation with a linear potential. The Wronskian and wave functions read:

$$\mathsf{W}[\mathrm{Ai}, \phi]\,(x) = \mathrm{Ai}(\xi)\,\phi'(x)\sqrt{\frac{m^*}{m}} - \sqrt{\frac{m}{m^*}}\mathrm{Ai}'(\xi)\,\xi'(x)\,\phi(x) \tag{9}$$

$$\phi^{\pm}_{iA}(x) = e^{\pm i k_{iA}(x - x_A)}, \qquad \phi^{\pm}_{iB}(x) = e^{\pm i k_{iB}(x - x_B)}, \qquad \xi(x) = J \cdot \left(x + \frac{a_0 - \varepsilon_i}{a_1}\right) \tag{10}$$

Obviously, the left-to-right $\tau_{\rightarrow}(\varepsilon_i)$ and right-to-left $\tau_{\leftarrow}(\varepsilon_j)$ transparencies differ if $\varepsilon_i \neq \varepsilon_j$. When a positive bias voltage is applied $V = V_R - V_L > 0$, we choose left-to-right transparencies $\tau_{\rightarrow}$ and vice versa.

As a result, all tunnel amplitudes $T_{ij\sigma}, T^{\zeta}_{\mathbf{ik}\sigma}$ can be derived from the geometric dimensions of the system (coordinates x^c_A, x^c_B, *etc.*) and the known band structure (Fermi energies, electron affinities, dopant ionisation potentials). However, the band structure may be strongly distorted in nanoscale systems, so we treat the potential well depths (E_A, E_B, *etc.*) as well as their coordinates (x^c_A, x^c_B, *etc.*) as free fitting parameters.

Coulomb energies

Now we discuss the last two Coulomb terms in the Hamiltonian eq (5). The main difference from generic terms like $U\hat{n}_\uparrow\hat{n}_\downarrow$ is that we explicitly introduce the reference filling factors $n^0_{i\sigma}$. These values correspond to the filling factors of the localisation sites the system would have in the electrically neutral configuration in the limit of the zero temperature. In the case of donor impurities $n^0_{i\sigma} = 1$ as these atoms are electrically neutral together with their valence electrons. In the course of electron transport donor dopants may lose their valence electron and become charged positively.

When the Coulomb terms with explicit reference filling factors are expanded, one obtains the standard form of Coulomb repulsion plus linear terms which affect the single-particle discrete energy levels $\varepsilon_{i\sigma}$ as follows:

$$\sum_{i\sigma}\tilde{\varepsilon}_{i\sigma}\hat{n}_{i\sigma} + \sum_i \tilde{U}_{ii}(\hat{n}_{i\uparrow} - \hat{1}n^0_{i\uparrow})(\hat{n}_{i\downarrow} - \hat{1}n^0_{i\downarrow}) + \sum_{i<j}\tilde{U}_{ij}(\hat{n}_i - \hat{1}n^0_i)(\hat{n}_j - \hat{1}n^0_j)$$
$$= \sum_{i\sigma}\varepsilon_{i\sigma}\hat{n}_{i\sigma} + \sum_i \tilde{U}_{ii}\hat{n}_{i\uparrow}\hat{n}_{i\downarrow} + \sum_{i<j}\tilde{U}_{ij}\hat{n}_i\hat{n}_j + const, \quad (11)$$

where $\varepsilon_{i\sigma} = \tilde{\varepsilon}_{i\sigma} - U_{i\bar{\sigma}}n^0_{i\bar{\sigma}} - \sum_{j\neq i}U_{ij}n^0_j$. We have generalised the latter expression by distinguishing *dynamic* Coulomb energies $\tilde{U}_{ij}$ from the *static* ones U_{ij} (which renormalise the original energy levels $\tilde{\varepsilon}_{i\sigma}$). Finally, we use the following expression for discrete energy levels of dopants:

$$\varepsilon_{i\sigma} = \tilde{\varepsilon}_{i\sigma} \; - \; \left(U_{ii}n^0_{i\bar{\sigma}} + \sum_{j\neq i}U_{ij}n^0_j\right) \; - \; e\alpha_G V_G, \quad (12)$$

which also includes electrostatic shift with common gate voltage V_G and electrostatic lever $\alpha_G = 0.22$ (estimated above from the characteristics of the undoped nanobridge). Generalisation of eq (12) is essential because it allows us to distinguish the discreteness of the original noninteracting energy levels due to quantum confinement $\tilde{\varepsilon}_{i\sigma}$ from the discreteness of actual energy levels $\varepsilon_{i\sigma}$ that account for Coulomb interaction and can be sensed in the experiment at least implicitly. The discreteness of the original energy levels $\Delta\tilde{\varepsilon}_{i\sigma} = \tilde{\varepsilon}_{i+1,\sigma} - \tilde{\varepsilon}_{i\sigma}$ can vary

from $\sim 1\,\mathrm{meV}$ for shallow impurity atoms to $\sim 100\,\mathrm{meV}$ for deep ones.

Similarly to the tunnelling interaction, we derive Coulomb energies U_{ij} from the geometric dimensions of the nanosystem. For this purpose, we use a hydrogen-like model of an impurity atom. Firstly, we expect the effective localisation lengths Δl_i to behave analogously to the Bohr radii, $\Delta l_i = \Delta l_0\,(i - i_0)^\alpha$, with $i_0 = 0$ for the left dopant and $i_0 = 2$ for the right one. The reference localisation length $\Delta l_0 = \Delta l_A = \Delta l_B$ for all fitted models. Index $\alpha = 2$ in the Bohr model, although one may try $\alpha < 2$ for the slower decrease of U_{ii}. Secondly, we approximate the three-dimensional stationary single-particle wave functions of localised electrons with Gaussian primitives according to their effective localisation lengths,

$$\phi_i(\mathbf{r}) = \exp\!\left(-\frac{(\mathbf{r}-\mathbf{R}_i)^2}{(\Delta l_i)^2}\right)\left(\frac{\sqrt{2/\pi}}{\Delta l_i}\right)^{\frac{3}{2}}, \tag{13}$$

where radius-vectors $\mathbf{R}_1 = \mathbf{R}_2 = (x_A^c\ 0\ 0)^\mathsf{T}$ and $\mathbf{R}_3 = \mathbf{R}_4 = (x_B^c\ 0\ 0)^\mathsf{T}$ define the geometric positions of both two-level dopants. Thirdly, it is straightforward to estimate the Coulomb energies as standard two-particle Coulomb integrals:

$$U_{ij} = \frac{e^2}{4\pi\epsilon\epsilon_0}\iint \mathrm{d}\mathbf{r}_1\,\mathrm{d}\mathbf{r}_2\,\frac{\phi_i^*(\mathbf{r}_1)\,\phi_i(\mathbf{r}_1)\,\phi_j^*(\mathbf{r}_2)\,\phi_j(\mathbf{r}_2)}{|\mathbf{r}_1-\mathbf{r}_2|} \tag{14}$$

We use the numerical routines from the[11] library to compute these Coulomb integrals for the arbitrary dopant positions and localisation lengths.

The resulting energy parameters $U_{ij}, \Gamma_{ij\sigma}^{\zeta}$ and $T_{ij\sigma}$, derived from the best-fit geometric dimensions of the devices based on As, K and P, are listed in Table 1.

Effective local temperature and classical fluctuations

As already mentioned in section Theoretical model, the discrete energy levels $\varepsilon_{i\sigma}$ are subject to fluctuations of the background charge and additional thermal noise due to the interaction between the localised electrons and substrate phonons. Rigorous treatment of these fluc-

Table 1: Values of the 2D×2L model parameters $U_{ij}, \Gamma^{\zeta}_{ij\sigma}$ and $T_{ij\sigma}$ for devices based on As, K and P, derived from the best-fit geometric dimensions.

Dopant	$\min(U_{ij})$ meV	$\max(U_{ij})$ meV	$\max(\Gamma^{\zeta}_{ij\sigma})$ meV	$\max(T_{ij\sigma})$ meV
As	5.7	22	0.015	1.9
K	30	120	0.069	2.5
P	4.3	17	15.2	2.0

tuations on the quantum level of theory is beyond the scope of our model. Therefore, we account for these fluctuations by classical averaging with the Boltzmann-like distribution:

$$I(V, V_G) = \int I(V, V_G, \boldsymbol{\varepsilon} + \boldsymbol{\delta\varepsilon}) \frac{\exp\left(-\frac{|\boldsymbol{\delta\varepsilon}|}{k_B T_{\boldsymbol{\delta\varepsilon}}}\right)}{Z} \,\mathrm{d}(\boldsymbol{\delta\varepsilon}), \quad Z = \int \exp\left(-\frac{|\boldsymbol{\delta\varepsilon}|}{k_B T_{\boldsymbol{\delta\varepsilon}}}\right) \mathrm{d}(\boldsymbol{\delta\varepsilon}), \quad (15)$$

where $I(V, V_G, \boldsymbol{\varepsilon} + \boldsymbol{\delta\varepsilon})$ is calculated in the regular way outlined in section Theoretical model but with the artificially altered 'fluctuated' discrete energy levels, $\varepsilon_{i\sigma} \mapsto \varepsilon_{i\sigma} + \delta\varepsilon_{i\sigma}$. Since we include $N = 4$ energy levels, sufficient averaging (typically 20 fluctuations for each ε_i independently) would drastically increase the number of calculations by a factor of 20^4. However, under our conditions, electronic transport is mainly affected by fluctuations of at most two energy levels at a time, thus we perform averaging only over them independently. For example, when the current flows predominantly through levels $\varepsilon_{2\sigma}$ and $\varepsilon_{4\sigma}$ we make 20^2 samples of type $\boldsymbol{\delta\varepsilon} = (0\ \delta\varepsilon_2\ 0\ \delta\varepsilon_4)^{\mathsf{T}}$ so that $|\boldsymbol{\delta\varepsilon}| = |\delta\varepsilon_2| + |\delta\varepsilon_4|$ in eq (15).

Apart from averaging energy levels fluctuations $\boldsymbol{\delta\varepsilon}$ we pay additional attention to the temperature in the Boltzmann factors in eq (15). From a physical point of view, the flow of electric current I of the order of several nanoamperes across the macroscopic bias voltage V through a nanoscale bridge leads to significant self-heating of the whole structure. This phenomenon has already been observed in previous experiments[12]. Consequently, it is reasonable to deduce the effective local temperature T in a self-consistent way rather than to assume a constant substrate temperature T_0 throughout the sample. Specifically, we suggest

a simple linear dependence of the effective local temperature on the dissipated power:

$$k_B T \mapsto k_B T(I,V) = k_B T_0 + \kappa\, IV, \tag{16}$$

with the temperature-to-power coefficient $\kappa \simeq 10\,\mathrm{mK/pW}$ taken as the lowest bound from the I-V curve fitting (the upper bound remains uncertain). Remarkably, this value is of the same order as one can estimate from [12], Fig. 5.

As a result, the averaging of the classical fluctuations broadens the current peaks on the I-V characteristics and thus improves the fitting accuracy. In addition, the self-consistent calculation of the effective local temperature makes the peak broadening non-uniform, which further increases the fitting accuracy.

References

(1) Zorin, E. I.; Pavlov, P. V.; Tetelbaum, D. I.; Khokhlov, A. F. Donor Properties and Diffusion of K in Si. *Sov. Phys. Semicond.* **1972**, *6*, 21.

(2) Zorin, E. I.; Pavlov, P. V.; Tetelbaum, D. I.; Khokhlov, A. F. Difference Between the Properties of Na and K Doped Si. *Sov. Phys. Semicond.* **1972**, *6*, 334.

(3) Korol, V. M.; Zastavny, A. V. Behavior of potassium implanted in silicon. *Sov. Phys. Semicond.* **1977**, *11*, 926.

(4) Sze, S. M.; Ng, K. K. *Physics of Semiconductor Devices*; John Wiley & Sons, 2006.

(5) Ref. 4, p. 23.

(6) Glodeanu, A. Helium-Like Impurities in Semiconductors. *Phys. Status Solidi B* **1967**, *19*, K43–K46.

(7) Saleh-Jahromi, A.; Moebs, W. Energy levels of the lithium atom. *Eur. J. Phys.* **1998**, *19*, 355–360.

(8) Lekner, J. Electrostatics of two charged conducting spheres. *P. Roy. Soc. A - Math. Phy.* **2012**, *468*, 2829–2848.

(9) Anderson, P. W. Localized Magnetic States in Metals. *Phys. Rev.* **1961**, *124*, 41–53.

(10) Kopchinskii, I. D.; Shorokhov, V. V. Nonequilibrium Diagram Technique Applied to the Electronic Transport via Tightly Bound Localized States. *Russ. Microelectron.* **2023**, *52*, S337–S351.

(11) Library for the evaluation of molecular integrals over Gaussian functions. `https://github.com/evaleev/libint`.

(12) Krupenin, V. A.; Lotkhov, S. V.; Scherer, H.; Weimann, T.; Zorin, A. B.; Ahlers, F.-J.; Niemeyer, J.; Wolf, H. Charging and heating effects in a system of coupled single-electron tunneling devices. *Phys. Rev. B* **1999**, *59*, 10778–10784.